UNIVERSITY OF NIŠ
The scientific journal **FACTA UNIVERSITATIS**
Series: **Mechanical Engineering** Vol.1, N° 5, 1998 pp. 581- 593
Editor of series: Nenad Radojković, e-mail: radojkovic@ni.ac.yu
Address: Univerzitetski trg 2, 18000 Niš, YU
Tel: +381 18 547-095, Fax: +381 547-950
http://ni.ac.yu/Facta

THE CHATTER VIBRATIONS IN METAL CUTTING - THEORETICAL APPROACH

UDC:621.91:621.3.018

Ivana Kovačić

University of Novi Sad, Faculty of Technical Sciences, Department of Mechanics
Trg Dositeja Obradovica 6, 21000 Novi Sad, Yugoslavia

Abstract. *In this paper an appearance of chatter vibrations in metal cutting is investigated. The model of the system is based on the predictive machine theory of shear zone model. Since the dynamic cutting force is strongly influenced by the variations of cutting parameters, the objective of present paper is to consider the variations of rake angle and shear angle during feeding rate change, and to propose modified nonlinear model of cutting force and, consequently, nonlinear analytical model of chatter. By analysing the analytical solution of the governing equation three kinds of oscillatory motion are found. For each of them the variations of cutting force component (thrust force) and rake angle as a function of time are obtained numerically.*

Key words: *metal cutting, chatter vibrations*

1. INTRODUCTION

Chatter vibrations belong to the class of self-excited vibrations, whose occurrence in metal cutting has a bad influence on surface finish and dimensional accuracy of the work-piece, tool life and even machine life. A significant number of investigations have been done on various mechanisms and characteristics of chatter. The cutting process with variable feed is one of the principles of arising of chatter vibrations. That results in the variable dynamic cutting force. The approach to this problem can be experimental and theoretical. The former is often used for supporting the latter, and for getting instructions for improvements of work. Theoretical models are usually derived from a shear zone model of chip formation [1,2] assuming steady-state cutting data. However, this feature is contradictory to the experimental and theoretical investigations [3-6], which showed that during oscillatory cutting some parameters are changing and, consequently, the cutting

Received July 30, 1998

force, too. Tobias and Fishwick [7] found the first analytical expression of the dynamic cutting force variation as a function of an incremental variation of the chip-thickness and feed velocity. Kainth [3] evolved a theory of steady-state orthogonal cutting by including the influence of both chip-thickness and the rake angle. Nigm et al. considered the variations in the cutting parameters: feed, rake angle and cutting speed on the basis of dimensional analysis [5,6]. Lin and Weng [8] envisaged the cutting force affected by the variation of shear angle. By the reason of fundamental properties of the process nonlinear analytical models are needed [9]. Two aspects of the non-linearity of the cutting force are studied. One of them is to consider the nonlinear cutting force due to higher order chip thickness variations [8,10-13], which ensures the experimentally proved finite amplitude of chatter. The other is to consider the multiple regenerative effects [14,15].

In spite of extensive theoretical investigations the complete analytical model of chatter has not been formed yet, by the reason of complex cutting phenomena. Therefore, fundamental studies of the mechanics of oscillatory cutting are extremely important.

In this paper the model based on ideal shear concept is modified by considering the angular oscillations in that plane in response to the variations of cutting parameters: feed, rake angle and shear angle. The nonlinear behavior is also included in the model.

2. Modeling of the thrust force

Let us discuss the orthogonal wave cutting process with a shear zone model of chip formation. For the simplicity of presentation, the system with a single degree of freedom (x-coordinate) is represented (Fig. 1.). Merchant [1] derived the relation for the cutting force component (thrust force) F_x as a function of cutting conditions, tool angles and the frictional condition between the tool and work-piece, i.e.:

$$F_x = sw\tau \frac{\sin(\beta-\alpha)}{\sin\varphi\cos(\varphi+\beta-\alpha)} \quad , \tag{1}$$

where: s – feed, w – cutting width, τ – shear stress, β – friction angle, α – rake angle, φ – shear angle.

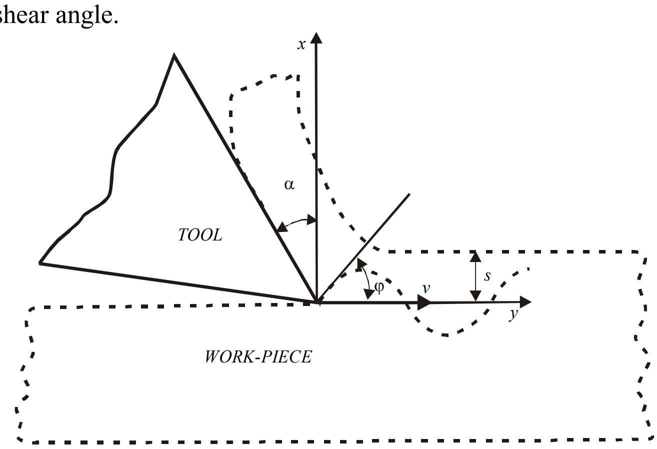

Fig. 1. Scheme of the orthogonal cutting process with continuous chip formation.

During oscillatory cutting process variations of the feed, rake angle and shear angle with respect to their steady-state values are expected. Let us denote these steady-state values with the subscripts 0. Thus, according to Fig.1, the instantaneous value of the feed is varied by small increment, which depends on the relative motion of the tool in x-direction, and takes the form:

$$s = s_0 - x\ . \tag{2}$$

Fig. 2. shows the variations of the rake angle α. It is easy to see that the change of this parameter is equivalent to the small angle ξ, which can be expressed as a function of the cutting speed v and the velocity of the tool vibration $\dot{x}$:

$$\xi = \arctan\left(\frac{-\dot{x}}{v}\right). \tag{3}$$

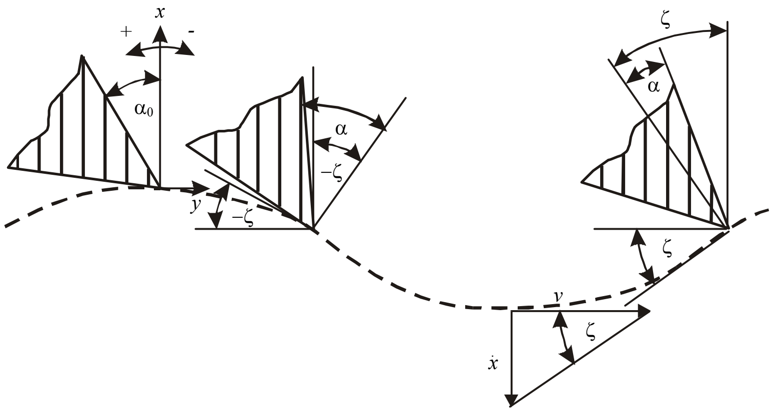

Fig. 2. Changing of the rake angle during the oscillatory cutting process.

Using the third order nonlinear form of angle ξ, the instantaneous value of the rake angle is obtained:

$$\alpha = \alpha_0 - \frac{\dot{x}}{v} + \frac{1}{3}\left(\frac{\dot{x}}{v}\right)^3. \tag{4}$$

For the case of wave cutting, such a change of the rake angle will result in the same change of the shear angle [6]. For our system this change is denoted by ξ, and we get the relation for the instantaneous value of the shear angle:

$$\varphi = \varphi_0 - \frac{\dot{x}}{v} + \frac{1}{3}\left(\frac{\dot{x}}{v}\right)^3. \tag{5}$$

The shear stress τ is slightly dependent on the cutting speed [5] and can be assumed as a constant value. The instantaneous value of the thrust force F_x is obtained by using the third-order Taylor's expansion in the neighborhood of steady-state values (s_0,α_0,φ_0) with respect to the incremental geometric variations. These variations are defined by the differences between the instantaneous values of the parameters: feed, rake angle and shear angle and steady-state ones. So,

$$F_x = F_{x0} - A_1 x - (B_1 + C_1)\frac{\dot{x}}{v} + \frac{E_1 + G_1 + J_1}{2}\left(\frac{\dot{x}}{v}\right)^2 + \left(\frac{B_1 + C_1}{3} - \frac{L_1 + M_1}{6} - \frac{Q_1 + S_1}{2}\right)\left(\frac{\dot{x}}{v}\right)^3$$
$$+ (H_1 + I_1)\frac{x\dot{x}}{v} - \left(\frac{P_1 + R_1}{2} + T_1\right)x\left(\frac{\dot{x}}{v}\right)^2 - \frac{H_1 + I_1}{3}x\left(\frac{\dot{x}}{v}\right)^3, \tag{6}$$

where coefficients of this expression are given in the Appendix.

3. Modeling of the tool vibrations

The equation of the motion of the tool can be written as:

$$m\ddot{x} + k\dot{x} + cx = F_x - F_{x0}\ , \tag{7}$$

where: m – equivalent mass of the system, $x \equiv d^2x/dt^2$, t – time
k – equivalent damping of the system, $\dot{x} \equiv dx/dt$, c–equivalent stiffness of the system
F_x is given by equation (6), and F_{x0} is the steady-state value of the thrust force.

3.1. Motions of the tool

In accordance to the paper [16] the solution in the first approximation for nonlinear ordinary differential equation (7), is:

$$x = a\cos\psi\ , \tag{8}$$

$$a = \frac{a(0)}{\sqrt{(1-b)\exp\left(t\cdot\frac{kv + B_1 + C_1}{mvf}\right) + b}}\ , \tag{9}$$

$$\psi = \psi_0 + t\left(\omega_1 + \frac{s_0 f k}{2vm\omega_1}\left[-\frac{B_1 + C_1}{2ms_0 f^2} + \right.\right.$$
$$\left.\left.\frac{a^2}{16}\left[\frac{(2B_1 + 2C_1 - L_1 - M_1 - 3Q_1 - 3S_1)s_0}{6mv^2} + \frac{(P_1 + R_1 + 2T_1)s_0 k}{mvf^2} + \frac{2(P_1 + R_1 + 2T_1)s_0}{mvf}\right]\right]\right) \tag{10}$$

where: a – the amplitude of vibrations, $a(0)$ – the initial amplitude

$$b = \frac{a^2(0)\left(\frac{(2B_1 + 2C_1 - L_1 - M_1 - 3Q_1 - 3S_1)s_0}{6v} + \frac{(P_1 + R_1 + 2T_1)k}{2(c + A_1)}\right)}{4\left(k + \frac{B_1 + C_1}{v}\right)}\ ,$$

ψ – the phase of vibrations, $\psi(0)$ – the initial phase,

$$\omega_1 = \sqrt{1-\left(\frac{k}{2mf}\right)}\ ,\ f = \sqrt{\frac{c+A_1}{m}}\ .$$

By analysing this solution the existence of three cases of motion can be identified. When the term, formed by damping coefficients of the equation of motion (7), is equal to zero, free oscillations of tool occur. This condition implies, so-called, the critical value of the cutting speed:

$$v_c = -\frac{s_0 w\tau}{k}\frac{\sin(\alpha_0-\beta)\cos(\alpha_0-\beta-2\varphi_0)-\sin\varphi_0\cos\varphi_0}{\sin^2\varphi_0\cos^2(\alpha_0-\beta-2\varphi_0)}\ . \tag{11}$$

For this value of the cutting speed we have the threshold of chatter. From the equation (9) it can be concluded that the amplitude of this motion a_I tends to its initial value:

$$a_I \to a(0)\ . \tag{12}$$

Second case is obtained for the cutting with the cutting speed v_{II}, which is higher than the critical value, i.e. for:

$$v_{II} > v_c\ , \tag{13}$$

the damped oscillatory motion occurs. The amplitude of the motion disappears:

$$a_{II} \to 0\ . \tag{14}$$

Finally, for the cutting system with the cutting speed v_{III}, which is smaller than the critical one:

$$v_{III} < v_c\ , \tag{15}$$

self-excited vibrations occur. The amplitude of this case a_{III} reaches the steady-state amplitude of this case a_{sIII}:

$$a_{III} \to a_{sIII} = \sqrt{\frac{4\left(k+\frac{B_1+C_1}{v}\right)}{\frac{(2B_1+2C_1-L_1-M_1-3Q_1-3S_1)s_0}{6v}+\frac{(P_1+R_1+2T_1)k}{2(c+A_1)}}} \tag{16}$$

Depending on the initial amplitude, there are two possibilities for system's behavior. When the initial amplitude $a(0)$ is smaller than the steady-state value a_{sIII}, the amplitude firstly increases and then becomes the constant value. When the initial amplitude is higher than the steady-state one, the amplitude firstly decreases and then reaches the same constant value a_{sIII}.

By applying the third-order Runge-Kutta numerical procedure to the equation (6) the existence of all analytically obtained cases of motion is proved. Results of this procedure in Fig. 3. are shown. In this paper dynamic behavior is investigated under the test conditions listed in the Table 1.

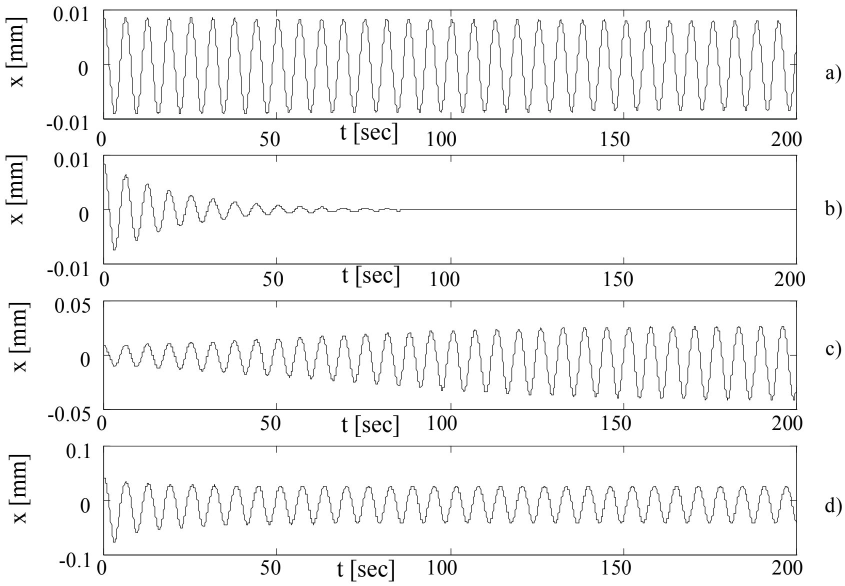

Fig. 3. Oscillatory motion of the tool:
a) free oscillations;
b) damped oscillations;
c) self-excited vibrations when $a(0) < a_{sIII}$;
d) self-excited vibrations when $a(0) > a_{sIII}$.

Table 1. Test conditions

equivalent mass of the system	$m = 15$ kg	shear stress	$\tau = 655\ 10^6$ Nm^{-2}
equivalent damping of the system	$k = 400$kg s^{-1}	friction angle	$\beta = 70^o$
equivalent stiffness of the system	$c = 3\ 10^6$ Nm^{-2}	rake angle (steady-state value)	$\alpha_0 = 10^o$
feed (steady-state value)	$s_0 = 0.17$ mm	shear angle (steady-state value)	$\varphi_0 = 10^o$
cutting width	$w = 2.5$ mm		
CASE I		$a(0) = 0.0085$ mm	
CASE II		$a(0) = 0.0085$ mm	
CASE III	$a(0) < a_{SIII}$	$a(0) = 0.0085$ mm	
	$a(0) < a_{SIII}$	$a(0) = 0.034$ mm	

3.2. Variations of the thrust force F_x

Of special interest is to analyse the variations of the thrust force F_x during the time for aforementioned cases. Namely, the dynamic cutting force excites the machine tool structure to generate the tool vibrations and as a consequence of these vibrations, the dynamic cutting force is in turn affected. In other words, the tool vibrations and dynamic cutting force form a well-known closed-loop system [12,17].

For this investigation the third-order Runge-Kutta numerical algorithm is used. Results of this procedure applied to the equations (7), (6) are plotted in Fig. 4.

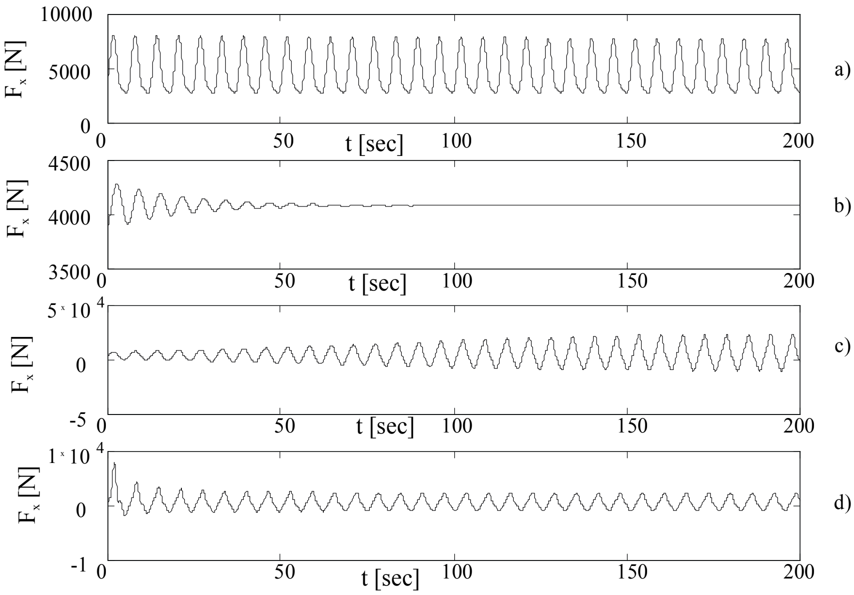

Fig. 4. Thrust force-time diagram:
a) for the case of free oscillations;
b) for the case of damped oscillations;
c) for the case of self-excited vibrations when $a(0) < a_{sIII}$;
d) for the case of self-excited vibrations when $a(0) > a_{sIII}$.

The effect and consequence of free vibrations of the tool is the thrust force, which varies harmonically with the constant value of the amplitude. So, according to the analytical solution (8), (12) and the equation (6) we have:

$$
\begin{aligned}
\sup remum\{F_{xI}\} = \max\Bigg(& \Bigg(F_{x0} + (B_1 + C_1)\frac{a(0)\dot{\psi}_I}{v_c} + \frac{E_1 + G_1 + J_1}{2}\left(\frac{a(0)\dot{\psi}_I}{v_c}\right)^2 - \left(\frac{2B_1 + 2C_1 - L_1 - M_1 - 3Q_1 - 3S_1}{6}\right)\left(\frac{a(0)\dot{\psi}_I}{v_c}\right)^3 \\
& - (H_1 + I_1)\frac{a^2(0)\dot{\psi}_I}{v_c} - \left(\frac{P_1 + R_1 + 2T_1}{2}\right)a(0)\left(\frac{a(0)\dot{\psi}_I}{vc}\right)^2 + \frac{H_1 + I_1}{3}a(0), \left(\frac{a(0)\dot{\psi}_I}{v_c}\right)^3\Bigg), \Bigg(F_{x0} - (B_1 + C_1)\frac{a(0)\dot{\psi}_I}{v_c} \\
& + \frac{E_1 + G_1 + J_1}{2}\left(\frac{a(0)\dot{\psi}_I}{v_c}\right)^2 + \left(\frac{2B_1 + 2C_1 - L_1 - M_1 - 3Q_1 - 3S_1}{6}\right)\left(\frac{a(0)\dot{\psi}_I}{v_c}\right)^3 - (H_1 + I_1)\frac{a^2(0)\dot{\psi}_I}{v_c} \\
& + \left(\frac{P_1 + R_1 + 2T_1}{2}\right)a(0)\left(\frac{a(0)\dot{\psi}_I}{v_c}\right)^2 + \frac{H_1 + I_1}{3}a(0), \left(\frac{a(0)\dot{\psi}_I}{v_c}\right)^3\Bigg)\Bigg),
\end{aligned}
\tag{17}
$$

where $\dot{\psi}_I$ is determined by equations (10)-(12).

The case of damped oscillations, when the amplitude a_{II} vanishes is obtained gratefully to the thrust force F_{xII}, which as $t \to \infty$, reaches the same value as the static elastic force F_{x0}, i.e.:

$$
F_{xII} \to F_{x0} = s_0 w \tau \frac{\sin(\beta - \alpha_0)}{\sin\varphi_0 \cos(\varphi_0 + \beta - \alpha_0)}. \tag{18}
$$

From the Fig. 4. and the Fig. 3. it is also seen that the self-excited variation of the thrust force causes the same kind of tool's motion. As $t \to \infty$, the thrust force F_{xIII} tends to constant value, which is not equal to the steady-state value F_{x0} :

$$\begin{aligned} \operatorname{sup}erior\{F_{xIII}\} \to \max\Bigg(& \Big(F_{x0} + (B_1 + C_1)\frac{a_{sIII}\dot{\psi}_{III}}{v_{III}} + \frac{E_1+G_1+J_1}{2}\left(\frac{a_{sIII}\dot{\psi}_{III}}{v_{III}}\right)^2 - \left(\frac{2B_1+2C_1-L_1-M_1-3Q_1-3S_1}{6}\right)\left(\frac{a_{SIII}\dot{\psi}_{III}}{v_{III}}\right)^3 \\ & -(H_1+I_1)\frac{a^2{}_{sIII}\dot{\psi}_{III}}{v_{III}} - \left(\frac{P_1+R_1+2T_1}{2}\right)a_{sIII}\left(\frac{a_{sIII}\dot{\psi}_{III}}{v_{III}}\right)^2 + \frac{H_1+I_1}{3}a_{sIII}\left(\frac{a_{sIII}\dot{\psi}_{III}}{v_{III}}\right)^3\Big), \Big(F_{x0} - (B_1+C_1)\frac{a_{sIII}\dot{\psi}_{III}}{v_{III}} \\ & + \frac{E_1+G_1+J_1}{2}\left(\frac{a_{sIII}\dot{\psi}_{III}}{v_{III}}\right)^2 + \left(\frac{2B_1+2C_1-L_1-M_1-3Q_1-3S_1}{6}\right)\left(\frac{a_{sIII}\dot{\psi}_{III}}{v_{III}}\right)^3 - (H_1+I_1)\frac{a^2{}_{sIII}\dot{\psi}_{III}}{v_{III}} \\ & + \left(\frac{P_1+R_1+2T_1}{2}\right)a_{sIII}\left(\frac{a_{sIII}\dot{\psi}_{III}}{v_{III}}\right)^2 + \frac{H_1+I_1}{3}a_{sIII}\left(\frac{a_{sIII}\dot{\psi}_{III}}{v_{III}}\right)^3\Big)\Bigg), \end{aligned} \tag{19}$$

where $\dot{\psi}_{III}$ is obtained on the basis of equations (10), (15), (16).

The linearized model for the thrust force has been included in the model of chatter for many researches. However, disadvantage of this consideration is that the linearized model does not correspond to the real one. Namely, the results of the linearized model show that the thrust force increases unlimited. This conclusion is affirmed in the Fig. 5., by comparing the results for linearized and nonlinear model of the thrust force for the condition given by equation (15), and $a(0) < a_{sIII}$.

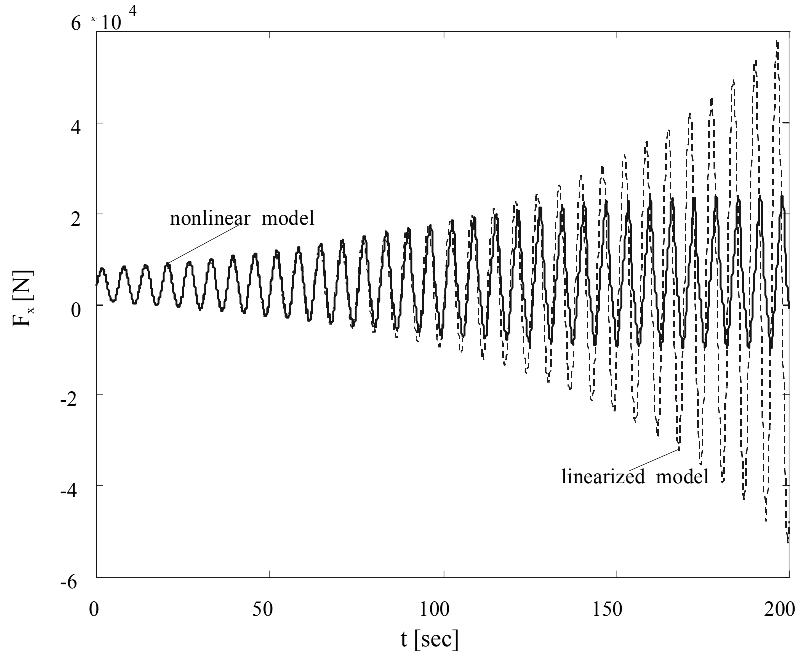

Fig. 5. Comparison of the values of thrust force:
linearized model (dotted line), nonlinear model (solid line).

3.3. Variations of the rake angle

When the dynamic cutting is investigated, variations of the shear angle are usually taken into consideration. But the change of the rake angle is very often neglected, and this angle is assumed as constant value α_0. Let us test accuracy of this statement. The investigation will be made by substituting numerically obtained solutions of the equation (7) into the equation (4). On the basis of comparison of the instantaneous values of the rake angle with the steady-sate one α_0, the relative error is plotted in the Fig. 6. For the case of free oscillatory motion of the tool, the rake angle α_I is changing between a minimum value α_{Imin} and maximum value α_{Imax} . For our test conditions when $\alpha_0 = 10^0$, the domain of the variation of the rake angle is defined by $\alpha_{Imin} \approx 4.28^0$ and $\alpha_{Imax} \approx 15.71^0$. These values indicate that the relative error is about 50%. For the case of damped vibrations of the tool, the value of rake angle α_{II} tends to the value α_0. However, at the beginning of the oscillatory cutting process the difference is about 2%. If the self-excited vibrations in the system occur, the rake angle α_{III} has the domain, which is determined with minimum α_{IIImin} and maximum α_{IIImax} . When $a(0) < a_{sIII}$, $\alpha_{IIImin} \approx -16.3^0$ and $\alpha_{IIImax} \approx 36.65^0$; while, when $a(0) > a_{sIII}$, $\alpha_{IIImin} \approx -25.85^0$ and $\alpha_{IIImax} \approx 48.49^0$.

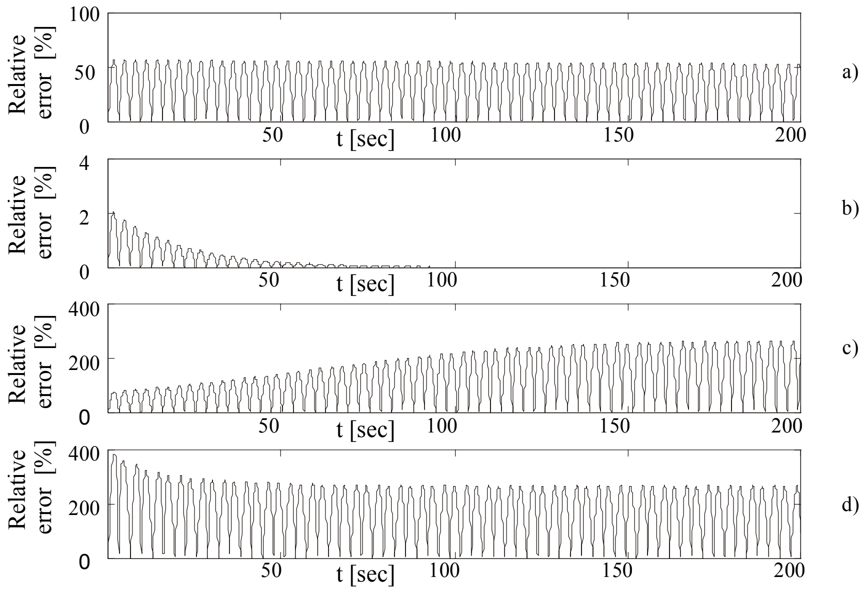

Fig. 6. Relative error of values of the rake angle as a function of the time:
a) for the case of free oscillations;
b) for the case of damped oscillations;
c) for the case of self-excited vibrations when $a(0) < a_{sIII}$;
d) for the case of self-excited vibrations when $a(0) > a_{sIII}$.

It is seen that for this case the difference is significant and can not be neglected.

4. CONCLUSIONS

It can be concluded:

- the motion of the tool is crucially affected by the cutting parameters. Depending on the value of the cutting speed with respect to its critical value given by equation (11) three cases can appear:
  - for the cutting process with the critical cutting speed (threshold of chatter) the tool oscillates with the constant amplitude.
  - when the cutting speed is higher than the critical one, the oscillatory motion of the tool disappears and only for this condition the steady-state cutting theory holds.
  - when the cutting speed is smaller than the critical value, the self-excited vibration occurs.

All these conclusions are completely in accordance to the previous experimental and theoretical observations, which state that chatter amplitude does not increase indefinitely but stabilizes at the finite value.

- by this non-linear model of chatter and non-linear model of thrust force, in which variations of the feed, rake angle and shear angle are included, representation of the oscillatory cutting system as a feedback loop is proved.
- there is a significant influence of occurrence of chatter on the variation of the rake angle for the case of free and self-excited vibrations and because of that its incremental change has to be included in the further investigations.

Acknowledgment - *The author would like to acknowledge that this project was co-supervised by Professor L. J. Cvetičanin.*

REFERENCES

1. M. E. Merchant, *Mechanics of the metal cutting process: orthogonal cutting and a type 2 chip*, J. Appl. Phys., Trans. ASME, vol. 16, pp. 267-275, 1945.
2. M. E. Merchant, *Mechanics of the metal cutting process: plasticity conditions in orthogonal cutting*, J. Appl. Phys., Trans. ASME, vol. 16, pp. 318-324, 1945.
3. G. S. Kainth, *Investigation into the dynamic of the metal cutting process*, Ph. D. dissertation, University of Birmingham, United Kingdom, 1969.
4. W. A. Knight, *Chatter in turning: some effects of tool geometry and cutting conditions*, Int. J. Mach. Tool Des. Res., vol 12, pp. 201-220, 1972.
5. M. M. Nigm, M. M. Sadek and S. A.Tobias, *Dimensional analysis of the seady state orthogonal cutting process*, Int. J. Mach. Tool Des. Res., vol. 17, pp.1-18 1977.
6. M. M. Nigm, M. M. Sadek and S. A. Tobias, *Determination of dynamic cutting coefficients from steady state cutting data*, Int. J. Mach. Tool Des. Res., vol. 17, pp. 19-37, 1977.
7. S. A. Tobias, and W. Fishwick, *The chatter of the lathe tool orthogonal cutting condition*, Trans. ASME J. Engng. Ind., vol. 80, No. 5., pp. 1079-1088, July 1958.
8. J. S. Lin, C. and I. Weng, *A nonlinear dynamic model of cutting*, Int. J. Mach. Tool Manufact., vol. 30, No. 1., pp. 53-64, 1990.
9. J. Gradisek, E. Govekar and I. Grabec, *A chaotic cutting process and determining optimal cutting parameter values using neural networks*, Int. J. Mach. Tool Manufact., vol. 36, pp. 1161-1172, 1996.
10. H. M. Shi and S. A. Tobias, *Theory of finite amplitude machine tool instability*, Int. J. Mach. Tool Des. Res., vol. 24, 45-69, 1984.
11. K. Jemelniak, and A. Widota, *Numerical simulation of non-linear chatter vibration in turning*, Int. J. Mach. Tools Manufact., vol. 29, No. 2., pp. 239-247, 1989.

12. Y. S. Tarng, H. T. Young and B. Y. Lee, *An analytical model of chatter vibration in metal cutting*, Int. J. Mach. Tools Manufact., vol. 34, No. 2., 183-197, 1994.
13. B. Y. Lee, Y. S. Tarng, and S. C. Ma, *Modeling of the process damping force in chatter vibration*, Int. J. Mach. Tool Manufact., vol. 35, No. 7., 951-962, 1995.
14. Y. Kondo, O. Kawano and H.Sato, *Behavior of self-excited chatter due to multiple regenerative effect*, Trans. ASME J. Engng. Ind., vol. 103, pp. 324-329, August 1981.
15. T. Kaneko, H. Sato, Y. Tani and M. O-hori, *Self-excited chatter and its marks in turning*, Trans. ASME J. Engng. Ind., vol. 106, pp. 222-228, August 1984.
16. I. Kovačić, *A new nonlinear dynamic model of chatter*, Submitted to Int. J. Mach. Tool Manufact.
17. H. E. Merrit, *Theory of self-excited machine tool chatter*, Trans. ASME J. Engng. Ind.Series B, vol. 87, No. 4., pp.447-454, 1965.

APPENDIX

The coefficients of the equation (6) are:

$$A_1 = w\tau \frac{\sin(\beta-\alpha_0)}{\sin\varphi_0 \cos(\varphi_0+\beta-\alpha_0)},$$

$$B_1 = s_0 w\tau \left\{ -\frac{\cos(\alpha_0-\beta)}{\cos(\alpha_0-\beta-\varphi_0)\sin\varphi_0} - \frac{\sin(\alpha_0-\beta)\sin(\alpha_0-\beta-\varphi_0)}{\cos^2(\alpha_0-\beta-\varphi_0)\sin\varphi_0} \right\},$$

$$C_1 = s_0 w\tau \left\{ -\frac{\cos\varphi_0 \sin(\alpha_0-\beta)}{\cos(\alpha_0-\beta-\varphi_0)\sin^2\varphi_0} + \frac{\sin(\alpha_0-\beta)\sin(\alpha_0-\beta-\varphi_0)}{\cos^2(\alpha_0-\beta-\varphi_0)\sin\varphi_0} \right\},$$

$$E_1 = s_0 w\tau \left\{ -\frac{2\cos(\alpha_0-\beta)\sin(\alpha_0-\beta-\varphi_0)}{\cos^2(\alpha_0-\beta-\varphi_0)\sin\varphi_0} - \frac{2\sin(\alpha_0-\beta)\sin^2(\alpha_0-\beta-\varphi_0)}{\cos^3(\alpha_0-\beta-\varphi_0)\sin\varphi_0} \right\},$$

$$G_1 = s_0 w\tau \left\{ -\frac{\sin(\alpha_0-\beta)\left[\dfrac{2\cos^2\varphi_0}{\sin^3\varphi_0} + \dfrac{2}{\sin\varphi_0}\right]}{\cos(\alpha_0-\beta-\varphi_0)} - \frac{2\cos\varphi_0 \sin(\alpha_0-\beta)\sin(\alpha_0-\beta-\varphi_0)}{\cos^2(\alpha_0-\beta-\varphi_0)\sin^2\varphi_0} \right.$$

$$\left. - \frac{2\sin(\alpha_0-\beta)\sin^2(\alpha_0-\beta-\varphi_0)}{\cos^3(\alpha_0-\beta-\varphi_0)\sin\varphi_0} \right\},$$

$$H_1 = w\tau \left\{ -\frac{\cos(\alpha_0-\beta)}{\cos(\alpha-\beta-\varphi_0)\sin\varphi_0} - \frac{\sin(\alpha_0-\beta)\sin(\alpha_0-\beta-\varphi_0)}{\cos^2(\alpha_0-\beta-\varphi_0)\sin\varphi_0} \right\},$$

$$I_1 = w\tau \left\{ \frac{\cos\varphi_0 \sin(\alpha_0-\beta)}{\cos(\alpha_0-\beta-\varphi_0)\sin\varphi_0} + \frac{\sin(\alpha_0-\beta)\sin(\alpha_0-\beta-\varphi_0)}{\cos^2(\alpha_0-\beta-\varphi_0)\sin\varphi_0} \right\},$$

$$J_1 = s_0 w\tau \left\{ \frac{\dfrac{\cos\varphi_0\cos(\alpha_0-\beta)}{\sin^2\varphi_0} + \dfrac{\sin(\alpha_0-\beta)}{\sin\varphi_0}}{\cos(\alpha_0-\beta-\varphi_0)} - \frac{\sin(\alpha_0-\beta-\varphi_0)\left[\dfrac{\cos(\alpha_0-\beta)}{\sin\varphi_0} + \dfrac{\cos\varphi_0\sin(\alpha_0-\beta)}{\sin^2\varphi_0}\right]}{\cos^2(\alpha_0-\beta-\varphi_0)} \right.$$

$$\left. - \frac{2\sin(\alpha_0-\beta)\sin^2(\alpha_0-\beta-\varphi_0)}{\cos^3(\alpha_0-\beta-\varphi_0)\sin\varphi_0} \right\},$$

$$L_1 = s_0 w\tau\left\{-\frac{2\cos(\alpha_0-\beta)}{\cos(\alpha_0-\beta-\varphi_0)\sin\varphi_0} - \frac{2\sin(\alpha_0-\beta-\varphi_0)\sin(\alpha_0-\beta-\varphi_0)}{\cos^2(\alpha_0-\beta-\varphi_0)\sin\varphi_0}\right.$$

$$\left.-\frac{6\cos(\alpha_0-\beta)\sin^2(\alpha_0-\beta-\varphi_0)}{\cos^3(\alpha_0-\beta-\varphi_0)\sin\varphi_0} - \frac{6\sin(\alpha_0-\beta)\sin^3(\alpha_0-\beta-\varphi_0)}{\cos^4(\alpha_0-\beta-\varphi_0)\sin\varphi_0}\right\},$$

$$M_1 = s_0 w\tau\left\{\frac{\sin(\alpha_0-\beta)\left[\frac{6\cos^3\varphi_0}{\sin^4\varphi_0}+\frac{8\cos\varphi_0}{\sin^2\varphi_0}\right]}{\cos(\alpha_0-\beta-\varphi_0)} + \frac{\sin(\alpha_0-\beta)\sin(\alpha_0-\beta-\varphi_0)\left[\frac{6\cos^2\varphi_0}{\sin^3\varphi_0}+\frac{8}{\sin\varphi_0}\right]}{\cos^2(\alpha_0-\beta-\varphi_0)}\right. +$$

$$\left.+\frac{6\cos\varphi_0\sin(\alpha_0-\beta)\sin^2(\alpha_0-\beta-\varphi_0)}{\cos^3(\alpha_0-\beta-\varphi_0)\sin^2\varphi_0} + \frac{6\sin(\alpha_0-\beta)\sin^3(\alpha_0-\beta-\varphi_0)}{\cos^4(\alpha_0-\beta-\varphi_0)\sin\varphi_0}\right\},$$

$$P_1 = w\tau\left\{-\frac{2\cos(\alpha_0-\beta)\sin(\alpha_0-\beta-\varphi_0)}{\cos^2(\alpha_0-\beta-\varphi_0)\sin\varphi_0} - \frac{2\sin(\alpha_0-\beta)\sin^2(\alpha_0-\beta-\varphi_0)}{\cos^3(\alpha_0-\beta-\varphi_0)\sin\varphi_0}\right\},$$

$$Q_1 = s_0 w\tau\left\{\frac{2\cos(\alpha_0-\beta)}{\cos(\alpha_0-\beta-\varphi_0)\sin\varphi_0} + \frac{\sin(\alpha_0-\beta-\varphi_0)\left[\frac{2\cos\varphi_0\cos(\alpha_0-\beta)}{\sin^2\varphi_0}+\frac{4\sin(\alpha_0-\beta)}{\sin\varphi_0}\right]}{\cos^2(\alpha_0-\beta-\varphi_0)}\right.$$

$$\left.+\frac{\sin^2(\alpha_0-\beta-\varphi_0)\left[\frac{4\cos(\alpha_0-\beta)}{\sin\varphi_0}+\frac{2\cos\varphi_0\sin(\alpha_0-\beta)}{\sin^2\varphi_0}\right]}{\cos^3(\alpha_0-\beta-\varphi_0)} + \frac{6\sin(\alpha_0-\beta)\sin^3(\alpha_0-\beta-\varphi_0)}{\cos^4(\alpha_0-\beta-\varphi_0)\sin\varphi_0}\right\},$$

$$R_1 = w\tau\left\{-\frac{\sin(\alpha_0-\beta)\left[\frac{2\cos^2\varphi_0}{\sin^3\varphi_0}+\frac{2}{\sin\varphi_0}\right]}{\cos(\alpha_0-\beta-\varphi_0)} - \frac{2\cos\varphi_0\sin(\alpha_0-\beta)\sin(\alpha_0-\beta-\varphi_0)}{\cos^2(\alpha_0-\beta-\varphi_0)\sin^2\varphi_0}\right.$$

$$\left.-\frac{2\sin(\alpha_0-\beta)\sin^2(\alpha_0-\beta-\varphi_0)}{\cos^3(\alpha_0-\beta-\varphi_0)\sin\varphi_0}\right\},$$

$$S_1 = -s_0 w\tau\left\{-\frac{\cos(\alpha_0-\beta)\left[\frac{2\cos^2\varphi_0}{\sin^3\varphi_0}+\frac{2}{\sin\varphi}\right]+\frac{2\cos\varphi_0\sin(\alpha_0-\beta)}{\sin^2\varphi_0}}{\cos(\alpha_0-\beta-\varphi_0)}\right. -$$

$$-\frac{\sin(\alpha_0-\beta-\varphi_0)\left[\frac{2\cos\varphi_0\cos(\alpha_0-\beta)}{\sin^3\varphi_0}+\sin(\alpha_0-\beta)\left[\frac{2\cos^2\varphi_0}{\sin^3\varphi_0}+\frac{6}{\sin\varphi_0}\right]\right]}{\cos^2(\alpha_0-\beta-\varphi)}$$

$$\left.-\frac{\sin^2(\alpha_0-\beta-\varphi_o)\left[\frac{2\cos(\alpha_0-\beta)}{\sin\varphi_0}+\frac{4\cos\varphi_0\sin(\alpha_0-\beta)}{\sin^2\varphi_0}\right]}{\cos^3(\alpha_0-\beta-\varphi)} - \frac{6\sin(\alpha_0-\beta)\sin^3(\alpha_0-\beta-\varphi_0)}{\cos^4(\alpha_0-\beta-\varphi_0)\sin\varphi_0}\right\},$$

$$T_1 = w\tau\left\{-\frac{\sin(\alpha_0-\beta)\left[\dfrac{2\cos^2\varphi_0}{\sin^3\varphi_0}+\dfrac{2}{\sin\varphi_0}\right]}{\cos(\alpha_0-\beta-\varphi_0)}-\frac{2\cos\varphi_0\sin(\alpha_0-\beta)\sin(\alpha_0-\beta-\varphi_0)}{\cos^2(\alpha_0-\beta-\varphi_0)\sin^2\varphi_0}-\right.$$

$$\left.-\frac{2\sin(\alpha_0-\beta)\sin^2(\alpha_0-\beta-\varphi_0)}{\cos^3(\alpha_0-\beta-\varphi_0)\sin\varphi_0}\right\}.$$

SAMOPOBUDNE OSCILACIJE U PROCESU REZANJA METALA - TEORIJSKI PRILAZ

Ivana Kovačić

Ovaj rad se bavi proučavanjem pojave samopobudnih oscilacija u procesu rezanja metala. Model sistema je baziran na teorijskom pristupu deformisanja metala u zoni smicanja. Kako je dinamička sila zavisna od vrednosti parametara rezanja, u ovom radu se razmatra uticaj koji na nju ima promena grudnog ugla i ugla smicanja tokom promene dubine rezanja, i formira modifikovani nelinearni model sile rezanja a, posledično, i nelinearni analitički model samopobudnih oscilacija. Analizom analitičkog rešenja utvrđeno je postojanje tri moguća slučaja oscilatornog kretanja alata. Za svaki od njih je numeričkim putem određena promena kompomnente sile rezanja (sile prodiranja) i grudnog ugla tokom vremena.